Available online at www.sciencedirect.com
ScienceDirect
Bioorganic & Medicinal Chemistry 15 (2007) 2106–2119
Bioorganic & Medicinal Chemistry

Benzoic acid and pyridine derivatives as inhibitors of *Trypanosoma cruzi trans*-sialidase

João Neres,[a] Pascal Bonnet,[a,†] Philip N. Edwards,[a] Pravin L. Kotian,[c] Alejandro Buschiazzo,[b] Pedro M. Alzari,[b] Richard A. Bryce[a] and Kenneth T. Douglas[a,*]

[a]*School of Pharmacy and Pharmaceutical Sciences, University of Manchester, Manchester, M13 9PL, UK*
[b]*Unité de Biochimie Structurale, Institut Pasteur, 25 rue du Dr. Roux, 75724 Paris, France*
[c]*BioCryst Pharmaceuticals, Inc., 2190 Parkway Drive, Birmingham, AL 35244, USA*

Received 3 October 2006; revised 7 December 2006; accepted 13 December 2006
Available online 15 December 2006

Abstract—Benzoic acid and pyridine derivatives inhibit recombinant *trans*-sialidase from *Trypanosoma cruzi* with I_{50} values between 0.4 and 1 mM. The best compounds, 4-acetylamino-3-hydroxymethylbenzoic acid and 5-acetylamino-6-aminopyridine-2-carboxylic acid, provide new leads to inhibitors not containing the synthetically complex sialic acid structure. The weak inhibition by such compounds contrasts with their much stronger inhibition of neuraminidase from Influenza virus.

1. Introduction

Chagas' disease, widely distributed in Central and South America with 13 million persons infected and 100 million people at risk, is estimated to cause 14,000 deaths annually. This disease is caused by *Trypanosoma cruzi*, a protozoan parasite transmitted to humans by haematophagous bugs or directly by transfusion of infected blood.[1] The only established drugs for the acute phase of infection are nifurtimox and benznidazole, with few other candidates yet on the clinical horizon.[2] The problem of resistance, both of the parasite to drug at molecular level and of the vector to insecticide, further adds to the gloomy prospects.[3] With this in mind there has been considerable interest in trying to develop novel approaches and targets for drug design.

A key problem in the pathogenicity of *T. cruzi* is its ability to evade host immune responses. Surface sialylation plays a central role in this and in the host cell adhesion/invasion mechanism, and provides a possible entry to novel therapeutics against this disease. This parasite is unable to synthesise sialic acids de novo. *Trans*-sialidase (TcTS), a parasite membrane-associated protein which catalyses the transfer of sialic acid molecules from host cell-surface glycoconjugates to its own surface mucin-like glycoproteins, seems to be a key enzyme to *T. cruzi* infective/invasive ability.[4–6] Thus, the developmental stage-specific expression of *trans*-sialidase is an important virulence factor of *T. cruzi*. As the *trans*-sialidases are unique to the parasite, TcTS has been discussed as a potential target for anti-Chagas drug design.[7,8] It is not possible to test the potential validity of this enzyme as a drug target by gene-knockout experiments as the TcTS protein family is coded for by 140 genes in the genome.[9] However, there are good biochemical reasons to believe that processes involving TcTS are vital to the parasite.

TcTS specifically (and preferentially) transfers sialic acid linked to saccharides or glycoconjugates by α-2,3 bonds to terminal β-galactosyl residues in acceptor molecules. However, in the absence of an appropriate acceptor, TcTS can also act as a sialidase, hydrolysing the donor substrate and releasing free sialic acid. Both activities (sialidase and *trans*-sialidase) are associated with the same active site in TcTS, therefore assays based on sialic acid transfer or hydrolysis can be used to monitor TcTS activity.[10–13]

There are no known specific chemical inhibitors of TcTS, nor drugs known to act against it. Thus, chemical

Keywords: *Trans*-sialidase; Inhibitors; Chagas disease; Neuraminidase.
* Corresponding author. Tel.: +44 161 275 2371; fax: +44 161 275 2481; e-mail: Ken.Douglas@manchester.ac.uk
† Present address: Johnson & Johnson Pharmaceutical Research & Development, Turnhoutseweg 30, 2340 Beerse, Belgium.

0968-0896/$ - see front matter © 2007 Elsevier Ltd. All rights reserved.
doi:10.1016/j.bmc.2006.12.024

evidence of the enzyme as a target is lacking, and the present contribution reports initial studies to discover novel inhibitory molecular architectures based on the availability of the crystal structure for this enzyme.[10] The crystal structure of TcTS shows two domains; the N-terminal catalytic domain is connected through a long α-helix to a C-terminal, lectin-like domain. The active site shows several of the conserved features of microbial sialidases, the main features being the arginine triad that binds the carboxylate group and a hydrophobic pocket that binds the *N*-acetyl group in sialic acid.[10]

The few inhibitors reported for TcTS are weak and have complex chemical structures. 2-Deoxy-2,3-didehydro-D-*N*-acetylneuraminic acid (DANA, **1**, Fig. 1), a potent inhibitor of Influenza neuraminidase, inhibits TcTS with a reported K_i of 12.3 mM.[14] The GM_3 ganglioside **2** is a good donor substrate for TcTS, but when the sialic acid residue is modified, namely at C4 (deoxy or methoxy), C7 (deoxy) and C8 (deoxy or methoxy), it becomes a partial inhibitor of the *trans*-sialidase reaction, at relatively high inhibitor/substrate ratios.[13]

2,3-Difluorosialic acid (**3**) inactivates TcTS time-dependently, through a covalent bond with the hydroxyl group of Tyr342. However, complete inactivation requires very high concentrations (20 mM) and the enzyme spontaneously recovers activity after removal of excess inactivator.[15] 3-Fluoro-sialosyl fluoride also covalently labels tyrosine for the sialidase from *T. rangeli* (~70% sequence identity for 640 aminoacids).[16] Although the enzymes from *T. cruzi* and *T. rangeli* show some similar features they behave distinctly from each other in their structural acceptance of various inhibitor frameworks.[17] Lactitol (**4**) and other lactose (acceptor substrate) analogues were reported to inhibit TcTS activity towards conventional substrates both in vitro and in vivo, again at relatively high concentrations of lactitol (mM range). However, these compounds do not inhibit the catalytic activity of TcTS but act as lpreferential acceptors when compared with the conventional β-galactosides.[18,19] Recently, two cyclohexenephosphonate monoalkyl esters **5** (I_{50} = 4.7 mM) and **6** (I_{50} = 5.7 mM) were also reported as weak inhibitors.[20]

Away from complex, sugar frameworks, the only report of TcTS inhibitors of which we are aware is pyridoxal phosphate (**7**, non-competitive inhibition, K_i 7.3 mM).[21] It has been pointed out that although strong inhibitors have been discovered against Influenza virus enzyme based on DANA, inhibitor design against the sialidases or *trans*-sialidases of bacteria or trypanosomes has been much less straightforward.[22] In view of this we now report the first generation of simple, non-sugar based inhibitors of TcTS that may lead to biological tools or potential leads for drug design. We address at this stage the sialic acid-binding site in TcTS.

One initial approach was to use a framework that had proved successful in the inhibition of Influenza virus neuraminidase.[23–27] This involved the replacement of the tetrahydropyran ring of sialic acid by simpler cyclic structures such as benzene or pyridine. With this approach, the relative chemical sensitivity and complex stereochemistry of the sialic acid or DANA-derived class of inhibitors is avoided, and one can begin to address issues such as bioavailability and other biologically important molecular properties. The compounds detected in this way also serve as initial frameworks to subsequently decorate with acceptor site ligand structures. We report TcTS inhibition data for a series of benzoic acid and pyridine-carboxylic acid derivatives (I and II, full structures are given in Tables 1 and 2, respectively), along with other carboxylic acid frameworks.

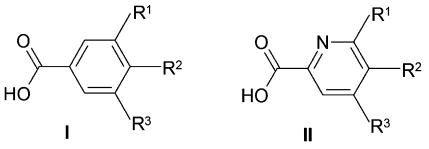

2. Results

2.1. Molecular modelling

2.1.1. Structure-based de novo design. The GRID program[28] was used to identify favourable energy

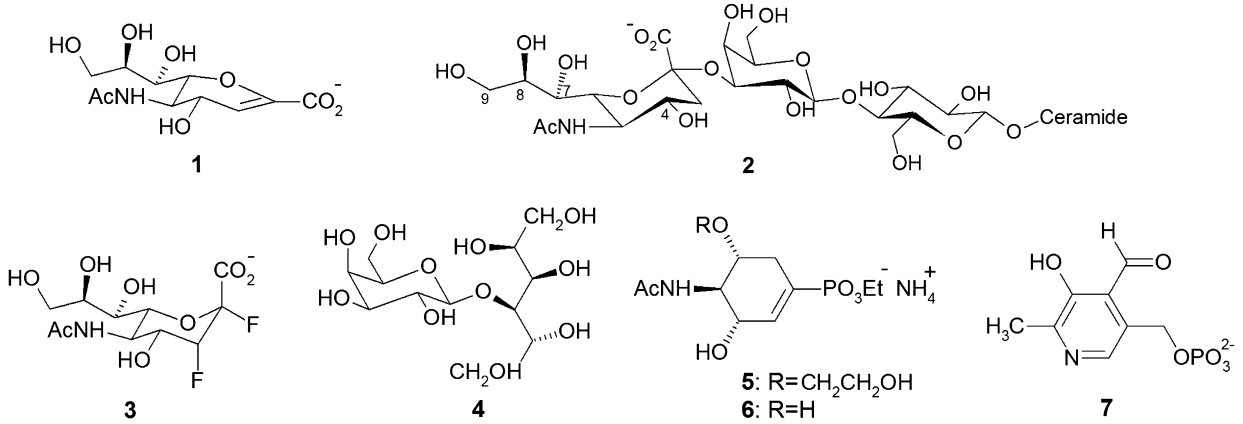

Figure 1. Structure of reported TcTS inhibitors.

Table 1. Inhibition of TcTS by benzoic acid derivatives I

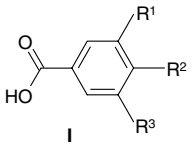

I

Code	R^1	R^2	R^3	Activity	
				% inhibition at 1 mM (±SD)	I_{50} (mM)
28	H	$NHCOCH_3$	H	0	—
29	CH_2OH	$NHCOCH_3$	H	—	0.54
30	CH_2CH_2OH	$NHCOCH_3$	H	16 ± 5	—
31[a]	$CH_2CH(OH)CH_2OH$	$NHCOCH_3$	H	17 ± 2	—
32[a]	$CH_2CH(OH)CH_2OH$	$NHCOCH_3$	H	0	—
33	$CH_2CH_2NH_2$	$NHCOCH_3$	H	25 ± 5	—
34	CH_2CONH_2	$NHCOCH_3$	H	0	—
35	CH=NOH	$NHCOCH_3$	H	24 ± 6	—
36	$N{=}C(NH_2)_2$	$NHCOCH_3$	H	41 ± 7	—
37	$N{=}C(NH_2)_2$	$NHCOCH_3$	CH_2CH_2OH	0	—
38	$N{=}C(NH_2)_2$	$CONHCH_3$	H	—	0.76
39	$N{=}C(NH_2)_2$	$NHSOCH_3$	H	29 ± 9	—
19	NH_2	$NHCOCH_2Ph$	H	—	1.2
18	$N{=}C(NH_2)_2$	$NHCOCH_2Ph$	H	54 ± 6[b]	—
8	$N{=}C(NH_2)_2$	$NHCH_2Ph$	H	9 ± 4	—
40	$N{=}C(NH_2)_2$	H	$CH_2CH_2NH_2$	[c]	—
41	$N{=}C(NH_2)_2$	$NHSO_2CH_3$	CH_2OH	11 ± 4	—
42	H	$NHSO_2CH_3$	$CH(OH)CH_2NH_2$	17 ± 2	—
43	$N{=}C(NH_2)_2$	$NHSO_2CH_3$	C=NOH	46 ± 7	—
44	$N{=}C(NH_2)_2$	H	$N{=}C(NH_2)_2$	[d]	—
45	$N{=}C(NH_2)_2$	H	C=NOH	35 ± 4	—
46	$N{=}C(NH_2)_2$	NH_2	CH_2CH_2OH	0	—
47	H	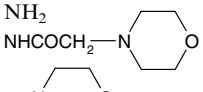	H	0	—
48	$NHCOCH_3$	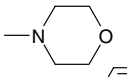	H	—	0.58
49	NH_2	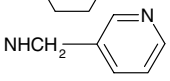	H	—	0.74
24	$N{=}C(NH_2)_2$	SCH_2Ph	H	43 ± 6[e]	—
25	NH_2	SCH_2Ph	H	—	0.70
27	$NHCOCH_2NH_2$	SCH_2Ph	H	—	1.0

[a] Compounds **31** and **32** are enantiomers.
[b] Concentration tested was 0.5 mM.
[c] Apparent activation (19% increase in activity).
[d] *Idem* (31%).
[e] Concentration tested was 0.4 mM.

Table 2. Inhibition of TcTS by pyridine-2-carboxylic acid derivatives II

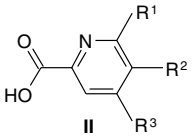

II

Code	R^1	R^2	R^3	Activity	
				% inhibition at 1 mM (±SD)	I_{50} (mM)
50	H	$NHCOCH_3$	H	22 ± 6	—
51	H	$NHCOCH_3$	NH_2	14 ± 6	—
52	NH_2	$NHCOCH_3$	H	—	0.44
53	H	$NHSO_2CH_3$	H	25 ± 12	—
54	H	$NHCSCH_3$	H	—	0.54

interaction regions in the active site between different functional group probes. As expected, the very strong interaction (−19 kcal/mol) of the carboxylate probe was detected in the region close to the arginine triad, as well as a favourable interaction with the cationic side chain of Arg93, as shown in Figure 2A where the structure of 2-deoxy-2,3-didehydro-D-*N*-acetylneuraminic acid (DANA) is superimposed in the crystallographic conformation in complex with TcTS.[10] The hydrophobic pocket formed by Trp120, Tyr113 and Val95 was clearly shown by various hydrophobic probes, including the methyl probe (Fig. 2B), and the DRY (hydrophobic probe) or the aromatic CH probe (not shown). This is the region which accommodates the *N*-acetyl group of DANA or sialic acid. Free space is available in the hydrophobic pocket, apparently enough to enclose groups as large as a phenyl ring.

The positively charged amidine probe, like other protonated nitrogen probes, gave essentially two regions with a strong interaction energy of −13 kcal/mol, between residues Glu230 and Asp96, and near Asp51 (Fig. 2C). Favourable binding positions at approximately −10 kcal/mol (Fig. 2D) were predicted for neutral NH or NH_2 probes in several regions of the active site, namely close to residues Glu230, Asp96 and Gln195 (binding region for the glycerol chain of DANA).

These results indicated target regions for positively charged groups, such as guanidino or protonated amino-acylamino groups (e.g., glycylamino), and also for hydrophobic groups to fit into the hydrophobic pocket. Benzoic acid derivatives were designed, replacing the sugar ring of sialic acid by a more synthetically accessible benzene ring, which would allow easier variation of the different substituent groups. This approach had proven successful for Influenza neuraminidase, with several benzoic acid-based sialic acid mimetics inhibiting the enzyme with I_{50} values in the low micromolar range, some even stronger.[23,29,30] Therefore, benzoic acid-derived structures were designed to contain these two functions *meta* and *para* to the carboxylate group. The structures of the designed compounds and all other compounds tested during the present work were docked into the active site using DOCK 4.0,[31] with ligand flexibility. Generally, the functional groups in the top-ranked docked poses obtained corresponded to the respective regions predicted by the GRID program.

Figure 3 shows the docked structures of **25** and **29** in the active site. The benzyl group of **25** was placed inside the hydrophobic pocket, adopting the favourable position predicted by GRID, and the amino group was hydrogen-bonded to both Asp96 and Glu230 (Fig. 3A). Docking of **29** gave a pose where the hydroxyl group was

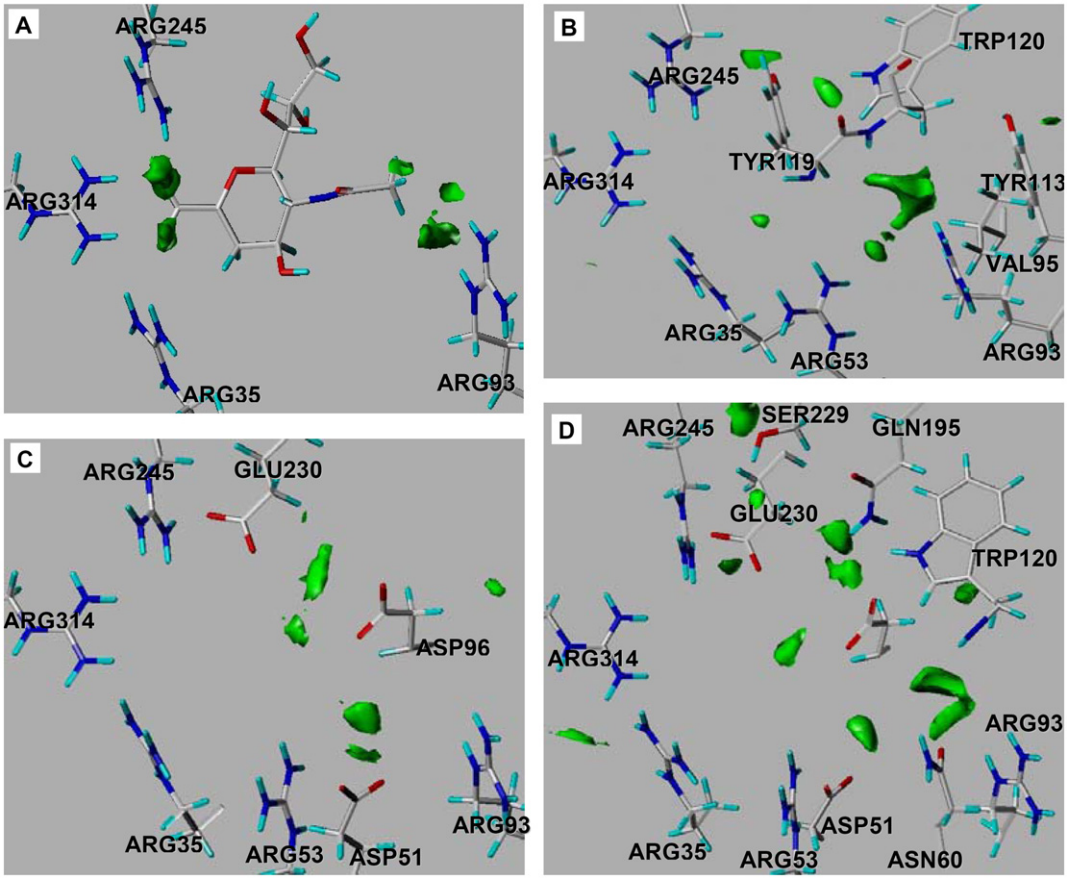

Figure 2. Favourable interaction energy surfaces (shown in green) obtained from the GRID program in the active site of TcTS. (A) Carboxylate probe (−19.0 kcal/mol) also showing DANA (crystallographic pose;[10]) (B) methyl probe (−4.0 kcal/mol); (C) neutral sp^3 NH probe (−10.5 kcal/mol); (D) cationic amidine probe (−13.5 kcal/mol).

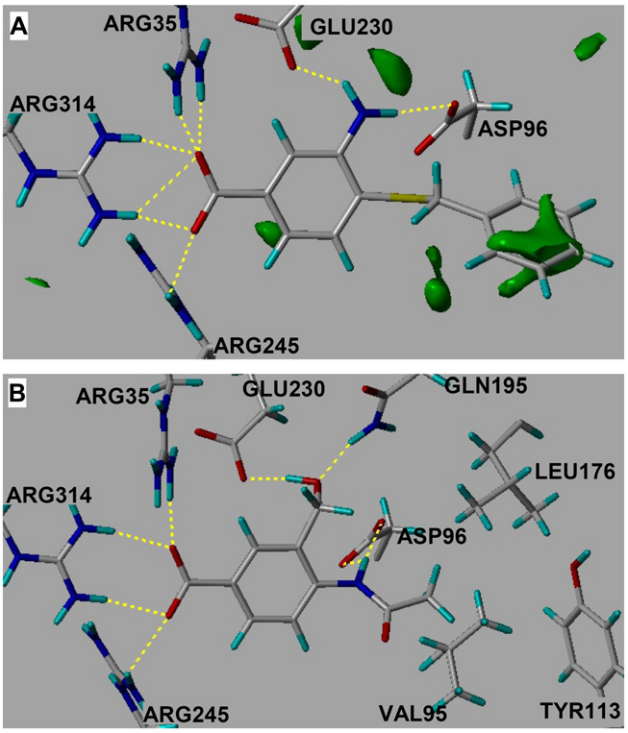

Figure 3. Docked conformation of compounds **25** (A), superimposed with the GRID favourable contour energy surface for the aromatic CH probe at −3.7 kcal/mol) and **29** (B) in the active site of TcTS.

hydrogen-bonded to both Gln195 and Glu230 and the amide nitrogen with Asp96 (Fig. 3B). Commonly to the observed for most benzoic acid derivatives studied in this work, in both structures the carboxylate group was in close interaction with the three arginine residues in the triad.

2.1.2. Virtual screening. Virtual screening of the Asinex database using DOCK produced numerous structurally diverse hits potentially containing negatively charged groups, such as carboxylate, sulfonamide and sulfone functions, predominantly positioned close to the arginine triad. Many also contained a positively charged group, usually interacting with one of the anionic residues in the active site, and/or a hydrophobic moiety, which was located in the hydrophobic pocket. Thus, the results of the screen are in line with the types of interactions seen in the preceding modelling work. Thirty-two highly ranked compounds with varied structural features were purchased from Asinex, with special attention given to benzoic acid and benzimidazole derivatives. However, only five of these compounds inhibited TcTS to some extent at 1 mM, namely **48**, **49** (Table 1) and **58**–**60** (Fig. 5). Results from virtual screening hits other than those shown in Table 1 (**47**–**49**) and Figure 5 (**57**–**60**) are not shown.

2.2. Synthesis

Benzoic acids **8**, **18** and **19** were synthesised from 4-amino-3-nitrobenzoic acid (**9**), according to Scheme 1. The methyl ester **10** was prepared to avoid side-reactions of the carboxylate group. Compound **11** was successfully synthesised in good yield (77%) by refluxing **10** in DMF for 70 h in the presence of excess benzyl bromide, even though the amine in the starting material was strongly deactivated by the *o*-nitro and *p*-carboxylic ester. Synthesis of **15** by reacting **10** with phenylacetyl chloride was more straightforward. Reduction of the nitro groups of **11** and **15** proceeded without problem using transfer hydrogenation, following the procedure described by Singh et al.[32] Whereas **17** was synthesised by reaction of **16** with cyanamide and HCl with 52% yield, the synthesis of **14** was performed with the strerically more demanding reagent, 1,3-bis(*tert*-butoxycarbonyl)-2-methyl-2-thiopseudourea, due to the presence of the additional benzyl-substituted amine group in **12**. The *t*-Boc groups of **13** were efficiently removed using triethylsilane and TFA in reasonable yield (68%), according to a method previously developed in our laboratory.[33] Hydrolysis of the methyl esters in NaOH yielded the target compounds in the neutral form (zwitterionic for **8** and **18**).

Synthesis of **24**, **25** and **27** (Scheme 2) started from the methyl ester of 4-chloro-3-nitrobenzoic acid (**20**) with introduction of the benzylmercaptyl group. Compound **24** was obtained after introduction of the guanidino group using the conditions used for **18**, followed by methyl ester hydrolysis. Fmoc-protected glycine was used to synthesise **26** from **22** in the presence of DCC. Fmoc group removal with diethylamine followed by ester hydrolysis gave **27**.

2.3. TcTS inhibition

TcTS inhibition screening results including I_{50} values for a series of substituted benzoic acid and pyridinecarboxylic acid derivatives are given in Tables 1 and 2, respectively. Inhibition results and structures for other compounds tested, including furosemide (**55**), are shown in Figure 5. The percentage inhibition at 1 mM concentration is the average of at least three independent experiments.

The inhibition by **29** was studied in greater detail to determine the inhibition pattern of diagnostic plots. The data are shown in Figure 4A–C. The lines, drawn by linear least squares regression analysis, are not fitted to either mixed or non-competitive kinetic inhibition models for this display. Fitting the data by non-linear least squares analysis to the respective equations for non-competitive and mixed inhibition models gave the following results, which were not significantly different, according to the statistical *F* test, performed in GRAFIT.[34] Non-competitive inhibition: K_i 0.33 ± 0.03 mM, K_m 0.73 ± 0.11, V_{max} 10,806 ± 870 fluorescence units (reduced χ^2 71,671); mixed inhibition: K_i 0.37 ± 0.17 mM, K_i' 0.31 ± 0.13 mM, K_m 0.75 ± 0.17, V_{max} 11,011 ± 1352 fluorescence units (reduced χ^2 75,068). Either model confirms the weak inhibition with K_i values around 300 μM.

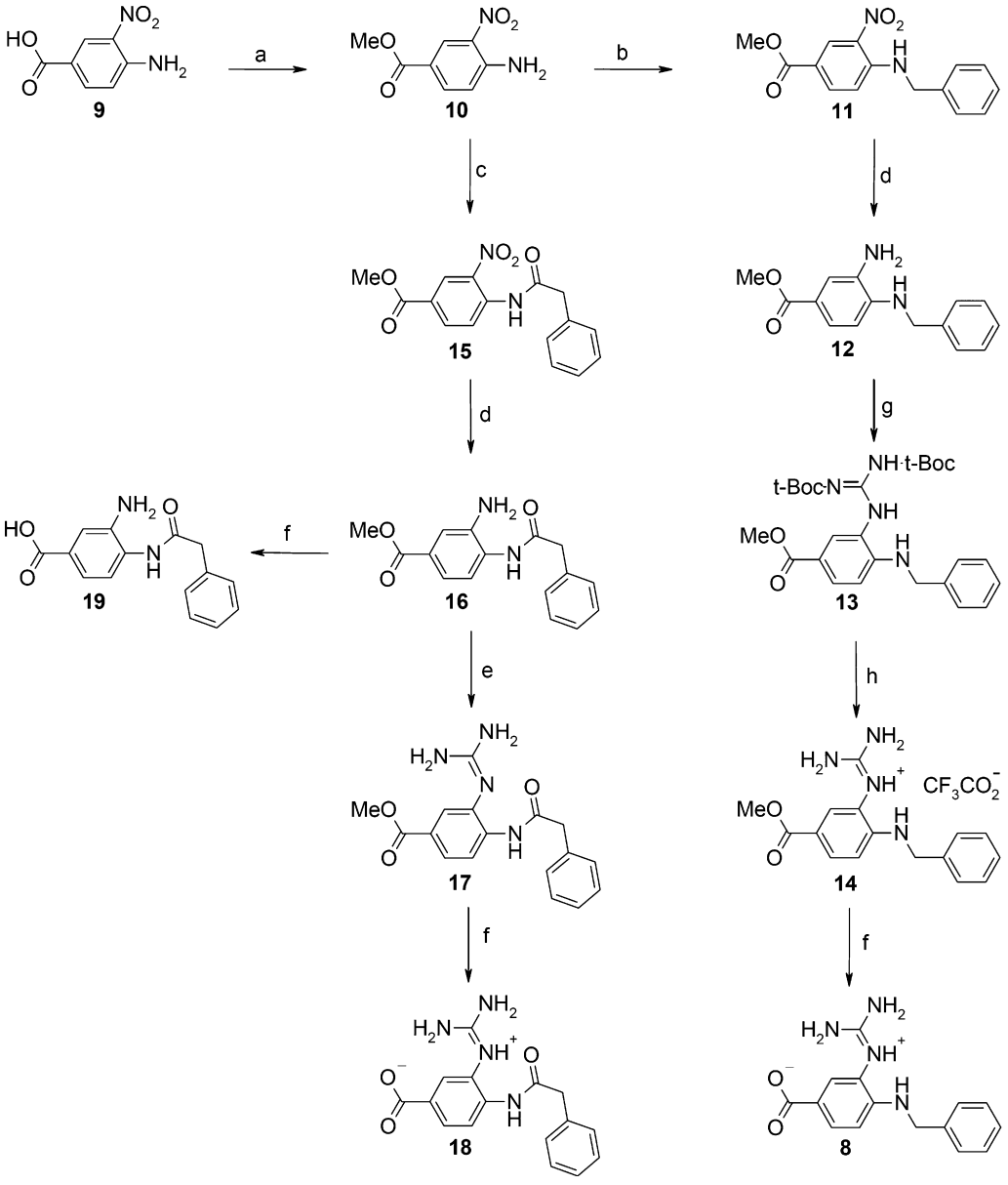

Scheme 1. Reagents and conditions: (a) MeOH, concd H_2SO_4, Δ; (b) $PhCH_2Br$, DMF, Δ; (c) $PhCH_2COCl$, $CHCl_3$, Δ; (d) H_2NNH_2, 10% Pd/C, EtOH; (e) H_2NCN, concd HCl, EtOAc, Δ; (f) 1—1 M NaOH; 2—HCl; (g) $H_3CSC[=NCO_2C(CH_3)_3]NHCO_2C(CH_3)_3$, Et_3N, $HgCl_2$, DMF; (h) TFA, Et_3SiH, DCM.

3. Discussion

Sialic acid derivatives/mimetics were highly successful in the design of inhibitors for the related Influenza neuraminidase, with the discovery of potent inhibitors, two of which are now in the market for the treatment of Influenza virus infections.[35,36] However, we have found in the present studies that the behaviour of the enzymes from Influenza and trypanosome is very different in respect of recognition of inhibitor structures.

In the present work, we used a sialic acid hydrolysis assay, previously validated in our laboratory,[11] to assess the inhibition of TcTS by the described compounds. We found a substantial difference in the behaviours of the substituted aromatic carboxylic acids from Tables 1 and 2 towards TcTS compared with the Influenza neuraminidase, with no apparent correlation between the two. For example, the stronger Influenza enzyme inhibitors **36**, **38**, **43** and **51** had I_{50} values of 2.5, 5, 80 and 70 μM, respectively, against this enzyme.[23,24] However with TcTS, inhibition was much weaker, with **36** and **43** inhibiting 40–50% of the activity at 1 mM and **51** only 14% inhibition at the same concentration, and **38** with an I_{50} of 0.76 mM. Conversely, stronger TcTS inhibitors **29** and **52**, with I_{50} of approximately 0.5 mM, were weaker inhibitors of the Influenza enzyme.[23,24] Compound **54** had a similar I_{50} for both enzymes (~0.4–0.5 mM).[24] In general, the strong inhibition that some aromatic carboxylates could achieve for the Influenza enzyme (with I_{50} values as low as 2.5 μM for **36**) was not observed for TcTS. The strongest TcTS inhibitors here described only showed I_{50} values in 0.4–1 mM region. The remaining aromatic

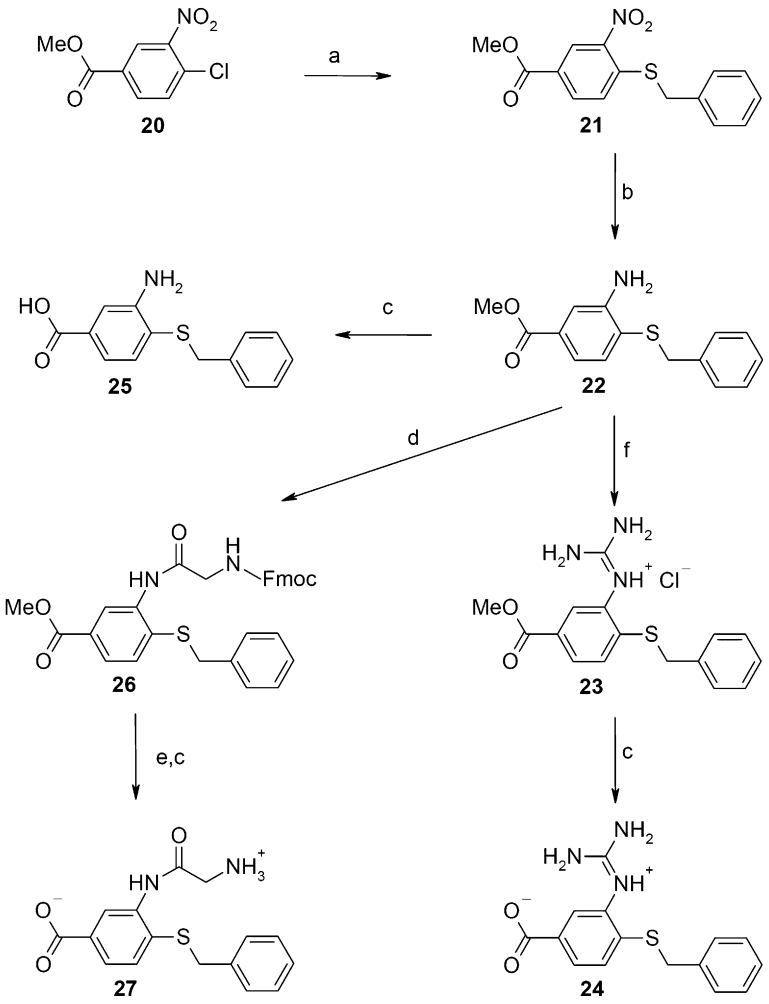

Scheme 2. Reagents and conditions: (a) $PhCH_2SH$, Na_2CO_3, Δ; (b) Fe, AcOH, EtOH, Δ; (c) 1—1 M NaOH; 2—HCl; (d) Fmoc-Gly-OH, DCC, DMF; (e) Et_2NH, EtOAc, Δ; (f) H_2NCN, concd HCl, EtOAc, Δ.

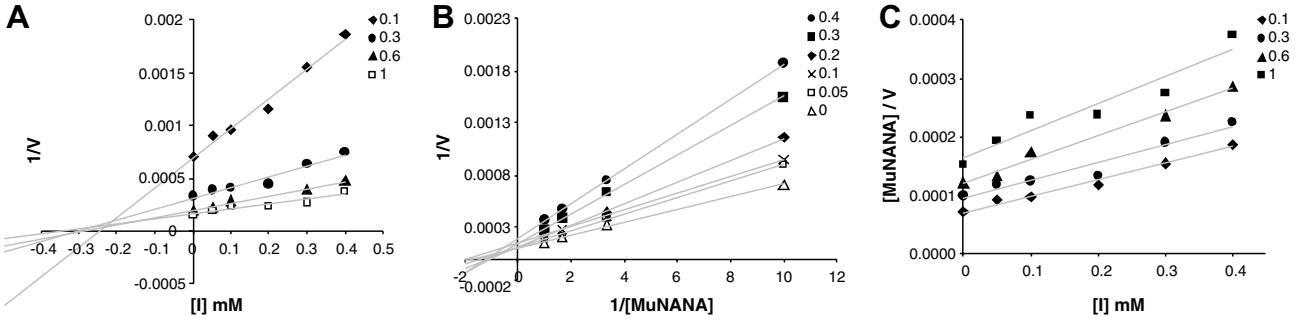

Figure 4. Graphical determination of the type of inhibition for compound **29**. (A) Dixon plot; (B) Lineweaver-burk plot; (C) Cornish-Bowden plot. Points are experimental; lines are by linear least squares regression analysis.

compounds are also weak inhibitors of Influenza neuraminidase, with I_{50} above 0.1 mM, in most cases even higher than 1 mM.[23,24,37]

Regarding TcTS inhibition of compounds in Table 1 with $R^2 = NHCOCH_3$, it is clear that we have been unable to recruit the potential cationic binding site of Figure 2C (Glu230 and Asp96) either using $CH_2CH_2NH_3^+$ (**33**) or a guanidino group (**36**). Replacing $R^2 = NHCOCH_3$ of **36** by $NHCOCH_2Ph$ (**18**) improved the percentage inhibition at 1 mM slightly, and going to $R^2 = NHCH_2Ph$ (**8**) substantially weakened inhibition, although this could be recovered by the SCH_2Ph replacement (**24**). For the $R^2 = SCH_2Ph$ family, replacing the R^1 guanidino group of **24** by NH_2 (**25**) or $NHCOCH_2NH_3^+$ (**27**) probably weakened the inhibi-

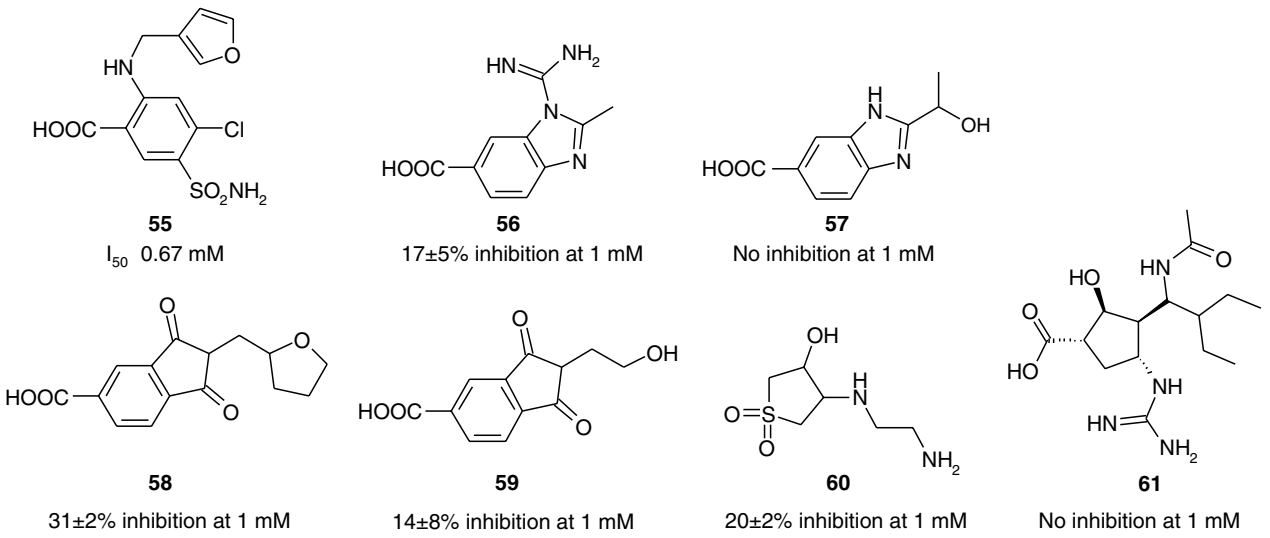

Figure 5. Structures and TcTS inhibition of other compounds tested.

tion slightly (with I_{50} values of 0.70 mM for **25** and 1.0 mM for **27**).

The inhibition by **29** is consistent with either non-competitive inhibition (K_i 0.33 ± 0.03 mM) or mixed inhibition (K_i 0.37 ± 0.17 mM, K_i' 0.31 ± 0.13 mM) with really very little to discriminate the models. In either case the inhibition is weak with K_i values around 300 μM only.

The introduction of a pyridine (Table 2) instead of a benzene nucleus (Table 1) made little difference to the strength of inhibition of TcTS (compare **28** and **50**). Compound **51** inhibits the Influenza enzyme with an I_{50} of 0.07 mM[24] but is much weaker with TcTS. Compound **61** is very strong against the Influenza enzyme (with I_{50} in the low nanomolar range), indeed reaching phase III clinical trials,[38] but was only a poor inhibitor of TcTS.

From the above data, it is clear that the Influenza and TcTS enzymes respond very differently to inhibitor structure. This can be explained not only by the structural differences between the two enzymes, but also by a different dynamic behaviour of sialidases and *trans*-sialidases.[14,17,39] Comparison of the crystal structures of Influenza neuraminidase (1F8B[40]) and TcTS shows many common features in the sialic acid-binding region, namely the arginine triad and Asp/Glu residues in approximately the same regions of the active site. However, the active site of the Influenza enzyme contains a greater number of negatively charged residues (Glu119, Asp151, Glu227, Glu276 and Glu277) when compared with TcTS (Asp59, Asp96, Glu230), plus there is one extra arginine residue (Arg53) in the latter. Furthermore, the active site of the Influenza enzyme (and indeed those of all structurally characterized sialidases, including the closely related *T. rangeli* enzyme) is easily accessible, with a greater solvent exposure than that in TcTS, where the active site is more hydrophobic. This is probably one key feature that distinguishes the different nature of the enzymatic activities, namely sialic acid hydrolysis for neuraminidase and sialic acid transfer for TcTS.[10] Another remarkable difference is the dynamic behaviour of TcTS during substrate binding and catalysis, where occupancy of the sialic acid-binding site was demonstrated to promote a conformational change that modulates the affinity for the acceptor sugar substrate.[10] Similar conformational changes are expected to take place upon inhibitor binding to the sialic acid-binding site. Although the nature and extent of these inhibitor-induced changes cannot be assessed in the absence of experimental structural information on TcTS-inhibitor complexes, it is plausible to suggest that they could be responsible for the lower sensitivity of *trans*-sialidase for the general sialidase inhibitor DANA[14] and might explain, at least in part, why it is difficult to obtain good TcTS inhibitors.

In particular, both the low accessibility and the flexible nature of the active site may account for the low activity of the aromatic carboxylate derivatives (Tables 1 and 2), since their docked structures fitted well in the active site of TcTS, with the guanidino and other positively charged groups interacting with the side chains of Glu230 and Asp96. Furthermore, these structures do not explore the acceptor substrate binding site in TcTS, which has been discussed as a potential target for TcTS inhibition and is targeted by lactitol and its derivatives, which prevent the sialylation of lactose or lactosamine by TcTS.[10,18,22]

The clinically used diuretic compound **55** (furosemide, Lasix®) also inhibits TcTS, but, with an I_{50} of 0.67 mM, any TcTS-based dose would be unacceptable in man. However, the furan ring region of **55** is docked against the acceptor substrate site in our docking analysis, thus providing an extra interaction with the active site compared with the other aromatic derivatives; further exploration of the SAR in this region is desirable.

In conclusion, the range of aromatic derivatives evaluated in the present work as TcTS inhibitors has shown the

possibility of inhibiting TcTS with this framework. Some of these compounds inhibit TcTS with I_{50} values in the high μM range (K_i value of ~300 μM for compound **29**), and while this is not of itself strong inhibition, they are the strongest inhibitors reported to date, with the exception of the extremely complex modified GM_3 ganglioside derivatives. Inhibition of TcTS by furosemide and the respective docked structure show that there is a possibility of including a substituent *ortho* to the carboxylate group in the aromatic ring, which binds the acceptor substrate binding site, thus offering room for improvement.

4. Experimental

4.1. Molecular modelling

The crystal structure of the TcTS–DANA complex[10] (PDB Accession code 1MS8) was used. Hydrogens were added using WHATIF,[41] with optimization of hydrogen bonds and determination of correct protonation state of histidine residues. The GREATER module of the GRID program[28] was used with default settings (grid resolution of 4 planes per Å) to screen the active site for energetically favourable binding regions for different functional group probes, thus giving further indications about the regions to target with newly designed inhibitors. Virtual screening on the Asinex Gold (~200,000 compounds) and Platinum (~100,000 compounds) databases (Asinex Ltd, Moscow, Russia) was performed with DOCK 4.0,[31] in two steps: the first step was rigid-body docking of all structures in the Asinex databases, with ligand minimization, testing a maximum of 1000 orientations for each molecule followed by minimization of the ligand docked pose. The DOCK 4.0 intermolecular scoring function was used to rank the ligands.[31] The top 320 scoring hits were then re-docked, now allowing flexibility of the ligand structure, using the torsion drive option for the conformational search and testing a maximum of 1000 orientations. Selection of compounds for in vitro inhibition assays was performed by visual inspection of the docked conformations resulting from the flexible-docking, using Sybyl 6.8.[42] Both virtual screening and de novo design targeted the sialic acid-binding site in TcTS. De novo design focused on benzoic acid derivatives with different substituents, as sialic acid mimetics. All compounds tested were docked in the active site using the flexible-docking algorithm as described for the second step of the virtual screening.

4.2. Chemistry: general procedures

Melting points, recorded in open capillary tubes in a Griffin melting point apparatus, and are uncorrected. ^{1}H NMR and ^{13}C NMR spectra were obtained in $CDCl_3$ or DMSO-d_6 with Me_4Si as internal standard on a Bruker Avance-300 Spectrometer operating at 300 MHz for ^{1}H NMR and 75 MHz for ^{13}C NMR. Exchangeable protons indicated by an asterisk were identified by D_2O shake. IR spectra were recorded on neat samples on a JASCO FT/IR 4100 with a PIKE/Miracle accessory. Electron ionisation (EI) and chemical ionisation (CI) mass spectra were recorded on a Micromass Trio 2000. Electrospray ionisation (ES) mass spectra were obtained using a Micromass Platform. High-resolution mass spectra were recorded using a Thermo Finnigan Mat 95 XP spectrometer. Elemental analyses were recorded on an EA 1108 Elemental Analyser (Carlo Erba Instruments) and were within 0.4% of the calculated values unless otherwise noted.

Compounds **29**–**46**, **50**–**54**, **56** and **61** were from previous studies by BioCryst Pharmaceuticals Inc. working on Influenza neuraminidase inhibitors.[23,24,37,38] Compounds **28** and **55** were purchased from Sigma–Aldrich (Gillingham, Dorset, UK) and **47**–**49** and **57**–**60** from Asinex Ltd, Moscow, Russia. Compound **10** was synthesised following a literature procedure[43] and the remaining compounds were synthesised as described below.

4.2.1. Methyl 4-benzylamino-3-nitrobenzoate (11). A mixture of **10** (8.0 g, 41 mmol), benzyl bromide (13.5 mL, 113 mmol) and DMF (15 mL) was heated at 70 °C for 3 days. The reaction mixture was diluted with CH_2Cl_2 (30 mL) and 1,4-diazabicyclo[2,2,2]octane (15.7 g, 94 mmol) added slowly with stirring at room temperature. Stirring was continued for 2 h and solvent was then evaporated in vacuo. The resulting residue was partitioned between EtOAc (100 mL) and 1 M citric acid (94 mL). The aqueous layer was washed with EtOAc (70 mL), the organic layers combined, dried over anhydrous Na_2SO_4 and evaporated to dryness in vacuo to give **11** (9.3 g, 79%) as a yellow solid: mp 98–100 °C (recryst from EtOH), lit. 98 °C.[44] ^{1}H NMR (DMSO-d_6): δ_H 3.81 (s, 3 H, OCH_3), 4.70 (d, J = 6.2 Hz, 2H, $C_6H_5CH_2$), 7.00 (d, J = 9.1 Hz, 1H, H5), 7.24–7.40 (m, 5H, $C_6H_5CH_2$), 7.9 (dd, J = 2.0 and 9.1 Hz, 1H, H6), 8.64 (d, J = 2.1 Hz, 1H, H2), 9.10* (t, J = 6.1 Hz, 1H, NH). ^{13}C NMR (DMSO-d_6): δ_C 46.1 ($C_6H_5CH_2$), 52.4 (OCH_3), 115.6 (C5), 116.4 (C1), 127.3 (C2′ and C6′), 127.5 and 128.7 (C2 and C4′), 129.0 (C3′ and C5′), 131.2 (C3), 135.9 (C6), 138.2 (C1′), 147.6 (C4), 165.1 (COOCH$_3$). MS (CI) m/z 287 ([M+H]$^+$, 100). HR-EI-MS (m/z) [M]$^+$ calcd for $C_{15}H_{14}N_2O_4$: 286.0954. Found: 286.0960. Anal. Calcd for $C_{15}H_{14}N_2O_4$: C, 62.9; H, 4.9; N, 9.8. Found: C, 63.0; H, 4.6; N, 9.6.

4.2.2. Methyl 3-amino-4-benzylaminobenzoate (12). A suspension of **11** (9 g, 31.4 mmol) in EtOH (25 mL) was added to a mixture of 10% Pd–C (3 g) and 5% HCl (7 mL). Hydrazine hydrate (85%, 4.4 mL, 120 mmol) dissolved in EtOH (10 mL) was then added drop-wise and the resulting mixture stirred for 2 h at room temperature. The reaction mixture was diluted with EtOH and EtOAc (20 mL of each), Pd–C was removed by filtration through Celite® and the filtrate concentrated under vacuum. The resulting residue was purified by column chromatography starting elution with CH_2Cl_2 with an increasing gradient of CH_2Cl_2:EtOAc. Fractions containing the product were combined and the solvent removed in vacuo. The residue obtained was recrystallised from MeOH yielding **12** as off-white crystals (4.9 g, 61%): mp 129–130 °C, lit.

125 °C.[44] ^{1}H NMR (DMSO-d_6): δ_H 3.70 (s, 3H, OCH_3), 4.38 (d, J = 5.8 Hz, 2H, $C_6H_5CH_2$NH), 4.85* (s, 2H, NH_2), 5.96* (br t, J = 5.7 Hz, 1H, $C_6H_5CH_2$NH), 6.35 (d, J = 8.3 Hz, 1H, H5), 7.10 (dd, J = 1.9 and 8.3 Hz, 1H, H6), 7.19 (d, J = 2.0 Hz, 1H, H2), 7.21–7.36 (m, 5H, $C_6H_5CH_2$NH). ^{13}C NMR (DMSO-d_6): δ_C 46.6 ($C_6H_5CH_2$NH), 51.5 (OCH_3), 108.9 and 114.8 (C2 and C5), 117.3 (C1), 120.9 (C6), 127.1 (C4′), 127.5 (C2′, C6′), 128.7 (C3′ and C5′), 134.4 (C3), 139.9 and 140.6 (C4 and C1′), 167.1 (COOCH$_3$). MS (ES$^+$) m/z 311 ([M+Na+MeOH]$^+$, 100), 279 ([M+Na]$^+$, 10), 257 ([M+H]$^+$, 23). Anal. Calcd for $C_{15}H_{16}N_2O_2$: C, 70.3; H, 6.3; N, 10.9. Found: C, 69.9; H, 6.2; N, 10.9.

4.2.3. Methyl 4-benzylamino-3-[*N*′,*N*″-di(*tert*-butoxycarbonyl)guanidino]benzoate (13). To an ice-cold suspension of **12** (1 g, 3.9 mmol) in dry DMF (7 mL) were added with stirring triethylamine (1.1 mL, 7.8 mmol), 1,3-*bis*-(*tert*-butoxycarbonyl)-2-methyl-2-thiopseudourea (1.7 g, 5.9 mmol) and $HgCl_2$ (1.6 g, 5.9 mmol). The ice bath was removed after 20 min and stirring continued at room temperature for 7 h. The reaction mixture was diluted with EtOAc (20 mL) and filtered through Celite®. Solvent was removed in vacuo and the residue obtained purified by column chromatography, starting with CH_2Cl_2 with an increasing gradient of CH_2Cl_2: EtOAc. Fractions containing the product were combined and solvent was removed in vacuo to give **13** as a white solid (1.2 g, 62%): mp 135–138 °C. ^{1}H NMR ($CDCl_3$): δ_H 1.44 (s, 9H, C(CH_3)$_3$), 1.54 (s, 9H, C(CH_3)$_3$), 3.84 (s, 3H, OCH_3), 4.43 (d, J = 5.8 Hz, 2H, $C_6H_5CH_2$NH), 5.64* (t, J = 5.7 Hz, 1H, $C_6H_5CH_2$NH), 6.64 (d, J = 8.4 Hz, 1H, H5), 7.25–7.37 (m, 5H, $C_6H_5CH_2$NH), 7.76–7.81 (m, 2H, H2 and H6), 9.97* (s, 1H, NHC(=NR)NHR), 11.61* (s, 1H, NHC(=NR)NHR). ^{13}C NMR ($CDCl_3$): δ_C 28.5 and 28.6 [2× (CH_3)$_3$], 48.1 ($C_6H_5CH_2$), 52.1 (OCH_3), 80.2 and 84.4 [2× C(CH$_3$)$_3$], 112.2 (C5), 119.0 (C1), 122.2 (C3), 127.6 (C4′), 127.8 (C2′ and C6′), 128.7 (C6), 129.1 (C3′ and C5′), 130.5 (C3), 138.8 (C1′), 147.7 (C4), 153.7 and 155.0 (2× C=O *t*-Boc), 163.5 (NHC(=NR)NHR), 167.2 (COOCH$_3$). MS (ES$^+$) m/z 499 ([M+H]$^+$, 100). Anal. Calcd for $C_{26}H_{34}N_4O_6$·0.25-H_2O: C, 62.1; H, 6.9; N, 11.1. Found: C, 62.2; H, 6.5; N, 11.1.

4.2.4. Methyl 4-benzylamino-3-guanidino-benzoate (14). To a solution of **13** (250 mg, 0.5 mmol) in dichloromethane (2 mL) were added trifluoroacetic acid (1 mL, 13 mmol) and triethylsilane (0.4 mL, 2.5 mmol). The reaction mixture was stirred at room temperature for 6 h with exclusion of moisture. Solvent was removed in vacuo, the residue triturated with chloroform and collected by filtration, and dried giving **14** as a white solid (0.14 g, 68%): mp 119–121 °C (recryst from MeOH/Et_2O). ^{1}H NMR (DMSO-d_6): δ_H 3.75 (s, 3H, OCH_3), 4.45 (d, J = 6.0 Hz, 2H, $C_6H_5CH_2$NH), 6.61 (d, J = 8.4 Hz, 1H, H5), 7.00* (t, J = 6.0 Hz, 1H, $C_6H_5CH_2$NH), 7.21–7.36 (m, 9H, C_6H_5 and NH=C(NH_2)$_2$), 7.56 (d, J = 1.8 Hz, 1H, H2), 7.68 (dd, J = 1.8 and 9.0 Hz, 1H, H6), 9.05* (s, 1H, NH=C(NH$_2$)$_2$). ^{13}C NMR ($CDCl_3$): δ_C 45.4 ($C_6H_5CH_2$), 51.4 (OCH_3), 110.6 (C5), 116.2 and 118.5 (C1 and C3), 126.7 (C2′, C4′ and C6′), 128.2 (C3′ and C5′), 130.3 and 130.9 (C2 and C6), 138.9 (C1′), 149.1 (C4), 156.8 (NH=C(NH$_2$)$_2$), 165.7 (COOCH$_3$). MS (ES$^+$) m/z 299 ([M+H]$^+$, 100). HR-ES-MS (m/z) [M+H]$^+$ calcd for $C_{16}H_{19}N_4O_2$: 299.1503. Found: 299.1500.

4.2.5. 4-Benzylamino-3-guanidino-benzoic acid (8). A mixture of **14** (80 mg, 0.19 mmol), 1 M NaOH (10 mL) and THF (1 mL) was stirred at 40 °C for 3 h. The resulting solution was concentrated in vacuo, diluted with water and the pH was adjusted to ~7 with 1 N HCl. The precipitate that formed was collected by filtration and dried, yielding **8** as a white solid (0.040 g, 73%). ^{1}H NMR (DMSO-d_6): δ_H 4.37 (br d, 2H, $C_6H_5CH_2$NH), 6.14* (br s, 1H, $C_6H_5CH_2$NH), 6.44 (d, J = 8.5 Hz, 1H, H5), 7.19 (t, J = 7.3 Hz, 1H, H4′), 7.28 (t, J = 7.3 Hz, 2H, H3′ and H5′), 7.40 (d, J = 7.3 Hz, 2H, H2′ and H6′), 7.53–7.56 (m, 2H, H2 and H6), 7.92* (br s, 4H, NH=C(NH_2)$_2$), 11.32* (br s, 1 H, NH=C(NH$_2$)$_2$). ^{13}C NMR (DMSO-d_6): δ_C 45.9 ($C_6H_5CH_2$), 109.7 (C5), 119.9 and 126.4 (C1 and C3), 126.5 (C4′), 126.9 (C2′ and C6′), 128.1 (C3′ and C5′), 128.6 and 129.2 (C2 and C6), 139.6 (C1′), 145.4 (C4), 157.3 (NH=C(NH$_2$)$_2$), 170.9 (COOH). MS (ES$^+$) m/z 285 ([M+H]$^+$, 100), 308 ([M+Na]$^+$, 48). HR-ES-MS (m/z) [M+H]$^+$ calcd for $C_{15}H_{17}N_4O_2$: 285.1346. Found: 285.1347.

4.2.6. Methyl 3-nitro-4-phenylacetylaminobenzoate (15). A mixture of **10** (1 g, 5.1 mmol) and phenylacetyl chloride (1.35 mL, 10.2 mmol) in $CHCl_3$ (2 mL) was stirred at 100 °C for 2 h. Acetonitrile (6 mL) was added to the reaction mixture, which was heated until the suspended solid dissolved. Water (1.5 mL) was added and the solution partitioned between CH_2Cl_2 (15 mL) and saturated $NaHCO_3$ solution (15 mL). The organic layer was separated, washed with water (2× 15 mL), dried over anhydrous Na_2SO_4 and solvent removed in vacuo. The residue was recrystallised from MeOH, yielding **15** (0.96 g, 60%) as a yellow solid: mp 129–130 °C. ^{1}H NMR ($CDCl_3$): δ_H 3.86 (s, 2H, $CH_2C_6H_5$), 3.94 (s, 3H, OCH_3), 7.35–7.47 (m, 5H, $CH_2C_6H_5$), 8.25 (dd, J = 2.0 and 8.9 Hz, 1H, H6), 8.83 (d, J = 2.0 Hz, 1H, H2), 8.94 (d, J = 8.9 Hz, 1H, H5), 10.48* (s, 1H, CONH). ^{13}C NMR ($CDCl_3$): δ_C 46.30 ($CH_2C_6H_5$), 53.02 (OCH_3), 121.92 (C5), 125.42 (C1), 127.86 and 128.60 (C2 and C4′), 129.88 (C3′ and C5′), 130.07 (C2′ and C6′), 133.21 and 135.93 (C3 and C4), 136.81 (C5), 138.52 (C1′), 165.04 (COOCH$_3$), 170.87 (CONH). MS (CI) m/z 315 ([M+H]$^+$, 100). HR-EI-MS (m/z) [M]$^+$ calcd for $C_{16}H_{14}N_2O_5$: 314.0903. Found: 314.0908. Anal. Calcd for $C_{16}H_{14}N_2O_5$: C, 61.1; H, 4.5; N, 8.9. Found: C, 61.2; H, 4.3; N, 8.9.

4.2.7. Methyl 3-amino-4-phenylacetylaminobenzoate (16). A suspension of **15** (0.7 g, 2.23 mmol) in EtOH (20 mL) was added to a mixture of 10% Pd–C (0.7 g) and 5% HCl (0.51 mL). Hydrazine hydrate (64%, 0.44 mL, 9.16 mmol) dissolved in ethanol (3 mL) was added drop-wise, and the mixture stirred for 1 h at room temperature, diluted with ethanol and ethyl acetate (20 mL of each) and the Pd–C removed by filtration through Celite®. The filtrate was evaporated in vacuo to give **16** as a white solid (0.52 g, 82%): mp 179–181 °C (recryst

from MeOH). ^{1}H NMR (DMSO-d_6): δ_H 3.70 (s, 2H, CH_2C$_6$H$_5$), 3.79 (s, 3H, OCH_3), 5.22* (s, 2H, NH_2), 7.15 (dd, J = 1.7 and 8.3 Hz, 1H, H6), 7.38 (d, J = 1.7 Hz, 1H, H2), 7.48 (d, J = 8.3 Hz, 1H, H5), 7.24–7.35 (m, 5H, CH$_2$C$_6$H$_5$), 9.46* (s, 1H, CONH). ^{13}C NMR (DMSO-d_6): δ_C 42.7 (CH$_2$C$_6$H$_5$), 51.7 (OCH$_3$), 116.3 and 117.2 (C2 and C6), 123.8 (C5), 126.2 (C1), 126.4 (C1 and C4′), 127.7 (C4), 128.2 (C3′ and C5′), 129.1 (C2′ and C6′), 135.9 (C1′), 140.8 (C3), 166.2 (COOCH$_3$), 169.3 (CONH). MS (CI) m/z 285 ([M+H]$^+$, 49). HR-EI-MS (m/z) [M]$^+$ calcd for C$_{16}$H$_{16}$N$_2$O$_3$: 284.1161. Found: 284.1160. Anal. Calcd for C$_{16}$H$_{16}$N$_2$O$_3$: C, 67.6; H, 5.7; N, 9.9. Found: C, 67.8; H, 5.5; N, 9.7.

4.2.8. Methyl 3-guanidino-4-phenylacetylaminobenzoate (17). A mixture of **16** (0.47 g, 1.65 mmol), cyanamide (1.4 g, 33 mmol) and concd HCl (0.15 mL) in EtOAc (15 mL) was refluxed for 6 h. The reaction mixture was diluted with EtOAc (30 mL) and partitioned with K_2CO_3 solution (15 mL, half of saturation concentration). The organic layer was washed with water, dried over Na_2SO_4, filtered and the solvent evaporated in vacuo. The residue obtained was recrystallised from EtOH yielding **17** (0.28 g, 52%) as a white solid: mp 182–184 °C. ^{1}H NMR (DMSO-d_6): δ_H 3.73 (s, 2H, CH_2C$_6$H$_5$), 3.77 (s, 3H, OCH_3), 5.48* (s, 4H, N=C(NH_2)$_2$), 7.24–7.40 (m, 6H, H6 and CH$_2$C$_6$H$_5$), 7.46 (d, J = 1.9 Hz, 1H, H2), 8.23 (d, J = 8.4 Hz, 1H, H5), 9.10* (s, 1H, CONH). ^{13}C NMR (DMSO-d_6): δ_C 43.98 (CH$_2$C$_6$H$_5$), 51.56 (OCH$_3$), 116.75, 121.18 and 121.21 (C2, C5 and C6), 123.65 (C1), 126.72 (C4′), 128.50 (C3′ and C5′), 129.28 (C2′ and C6′), 135.25 and 136.11 (C4 and C1′), 139.06 (C3), 154.39 (N=C(NH$_2$)$_2$), 166.35 (COOCH$_3$), 168.62 (CONH). MS (CI) m/z 327 ([M+H]$^+$, 100), 267 ([M−NH=C(NH$_2$)$_2$]$^+$, 45). HR-EI-MS (m/z) [M]$^+$ calcd for C$_{17}$H$_{18}$N$_4$O$_3$: 326.1379. Found: 326.1386. Anal. Calcd for C$_{17}$H$_{18}$N$_4$O$_3$·0.6H$_2$O: C, 60.4; H, 6.0; N, 16.6. Found: C, 60.2; H, 5.5; N, 16.9.

4.2.9. 3-Guanidino-4-phenylacetylaminobenzoic acid (18). A mixture of **17** (80 mg, 0.18 mmol), NaOH 1 M (0.6 mL) and THF (0.4 mL) was stirred at room temperature for 2 h. The pH of the resulting clear solution was adjusted to ~7 with 1 M HCl, and **18** precipitated as a white solid, which was collected by filtration and dried (0.059 g, 77%): mp 236–237 °C. ^{1}H NMR (DMSO-d_6): δ_H 3.73 (s, 2H, C$_6$H$_5$CH_2), 7.21–7.36 (m, 5H, C$_6$H$_5$), 7.71–7.79 (m, 3H, H2, H5, H6), 8.05* (br s, 4H, N=C(NH_2)$_2$), 10.0* (s, 1H, NHCOCH$_2$C$_6$H$_5$), 10.73* (br, COOH). MS (ES$^+$) m/z 313 ([M+H]$^+$, 100), 335 ([M+Na]$^+$, 52). HR-ES-MS (m/z) [M+H]$^+$ calcd for C$_{16}$H$_{17}$N$_4$O$_3$: 313.1295. Found: 313.1307.

4.2.10. 3-Amino-4-phenylacetylaminobenzoic acid (19). A mixture of **16** (20 mg, 0.070 mmol), NaOH 0.5 M (1 mL) and THF (0.5 mL) was stirred at room temperature for 16 h. The resulting suspension was filtered, the filtrate diluted with 2 mL of water and the pH adjusted to ~7 with 1 M HCl. The precipitate thus formed was collected by filtration and dried, giving **19** as a fine white powder (0.011 g, 58%): mp 168–170 °C. ^{1}H NMR (DMSO-d_6): δ_H 3.70 (s, 2H, C$_6$H$_5$CH_2CONH), 5.18* (s, 2H, NH_2), 7.12 (d, J = 8.2 Hz, 1H, H5), 7.23–7.34 (m, 6H, H2 and C$_6$H$_5$CH$_2$CONH), 7.43 (d, J = 8.2 Hz, 1H, H6), 9.50* (s, 1H, C$_6$H$_5$CH$_2$CONH), 12.56* (br s, 1H, COOH). ^{13}C NMR (DMSO-d_6): δ_C 42.7 (C$_6$H$_5$COCH$_2$), 116.6, 117.4 and 123.7 (C2, C5 and C6), 126.4 (C4′), 127.2 and 127.8 (C1 and C4), 128.2 (C2′ and C6′), 129.0 (C3′ and C5′), 136.0 (C1′), 140.7 (C3), 167.4 (C$_6$H$_5$CH$_2$$C$ONH), 169.2 ($C$OOH). MS (ES$^-$) m/z 269 ([M−H]$^-$, 100). HR-EI-MS (m/z) [M+Na]$^+$ calcd for C$_{15}$H$_{14}$N$_2$O$_3$Na: 293.0897. Found: 293.0893.

4.2.11. Methyl 3-nitro-4-benzylmercaptobenzoate (21). To a mixture of benzyl mercaptan (3.3 mL, 27.8 mmol), Na_2CO_3 (3.25 g, 30.6 mmol) and water (10 mL) was added methyl 4-chloro-3-nitrobenzoate (5 g, 23.2 mmol) in ethanol (40 mL). The mixture was refluxed for 2 h and diluted with water (40 mL). The solid thus formed was filtered off, washed with *n*-hexane and dried, yielding **21** as a yellow solid (6.56 g, 93%): mp 136–138 °C (recryst from MeOH), lit. 138 °C.[45] ^{1}H NMR (DMSO-d_6): δ_H 3.90 (s, 3H, OCH_3), 4.45 (s, 2H, C$_6$H$_5$CH_2S), 7.28–7.40 (m, 3H, H2′, H4′ and H6′), 7.47–7.50 (m, 2H, H3′ and H5′), 7.90 (d, J = 8.6 Hz, 1H, H5), 8.17 (dd, J = 1.9 and 8.6 Hz, 1H, H6), 8.64 (d, 1H, J = 1.9 Hz, H2). ^{13}C NMR (DMSO-d_6): δ_C 36.0 (C$_6$H$_5$$CH_2$S), 52.6 (O$CH_3$), 126.1 (C1), 126.4, 127.6 and 127.8 (C2, C5 and C4′), 128.6 (C2′ and C6′), 129.3 (C3′ and C5′), 133.4 (C6), 134.9 (C4), 142.8 (C1′), 144.5 (C3) and 164.3 (COOCH$_3$). MS (CI) m/z 321 ([M+NH$_4$]$^+$, 100), (EI) m/z 303 ([M]$^+$, 21). Anal. Calcd for C$_{15}$H$_{13}$NO$_4$S: C, 59.4; H, 4.3; N, 4.6; S, 10.6. Found: C, 59.1; H, 4.3; N, 4.6; S, 10.3.

4.2.12. Methyl 3-amino-4-benzylmercaptobenzoate (22). A solution of **21** (5 g, 16.5 mmol) in EtOH (10 mL) was treated with iron dust (7.9 g, 137 mmol) and 20% aqueous acetic acid (2.8 mL) refluxed for 30 min with vigorous stirring. The reaction mixture was diluted with EtOAc (40 mL) and filtered over Celite®. The filtered solution was washed with 5% aqueous $NaHCO_3$ (40 mL), followed by water (2× 40 mL), and dried over anhydrous Na_2SO_4. The solvent was evaporated in vacuo and the residue obtained was recrystallised from MeOH to give **22** as an off-white solid (4.0 g, 88%): mp 76–77 °C lit. 76–78 °C.[45] ^{1}H NMR (DMSO-d_6): δ_H 3.79 (s, 3H, OCH_3), 4.10 (s, 2H, C$_6$H$_5$CH_2S), 5.46* (s, 2H, NH_2), 7.05 (dd, J = 1.9 and 9.0 Hz, 1H, H6), 7.19–7.28 (m, 6H, H5 and C$_6$H$_5$CH$_2$S), 7.32 (d, J = 1.9 Hz, 1H, H2). ^{13}C NMR (DMSO-d_6): δ_C 36.3 (C$_6$H$_5$$CH_2$S), 51.8 (O$CH_3$), 114.3 and 116.6 (C2 and C6), 122.7 (C4), 127.0 (C4′), 128.2 (C2′ and C6′), 128.8 (C3′ and C5′), 128.9 (C1), 131.7 (C5), 137.4 (C1′), 147.7 (C3), 166.3 (COOCH$_3$). MS (CI) m/z 274 ([M+H]$^+$, 100). Anal. Calcd for C$_{15}$H$_{15}$NO$_2$S: C, 65.9; H, 5.5; N, 5.1; S, 11.7. Found: C, 66.0; H, 5.6; N, 5.1; S, 11.4.

4.2.13. Methyl 4-benzylmercapto-3-guanidino-benzoate hydrochloride (23). A mixture of **22** (0.7 g, 2.6 mmol), cyanamide (2.7 g, 64 mmol) and concd HCl (0.33 mL) in EtOAc (20 mL) was refluxed for 2 h. The reaction mixture was cooled to room temperature and a solid crystallised. This solid was filtered, washed with EtOAc and

dried, yielding **23** as a white solid (0.8 g, 88%): mp 245–246 °C (recryst from EtOH). ^{1}H NMR (DMSO-d_6): δ_H 3.85 (s, 3H, OCH_3), 4.36 (s, 2H, $C_6H_5CH_2S$), 7.26–7.48 (m, 9H, decreased to 5H after D_2O shake, $C_6H_5CH_2S$, NH=C(NH_2)$_2$), 7.62 (d, J = 8.4 Hz, 1H, H5), 7.73 (d, J = 1.8 Hz, 1H, H2), 7.90 (dd, J = 1.8 and 8.4 Hz, 1H, H6), 9.66* (br s, 1H, NH=C(NH_2)$_2$). ^{13}C NMR (DMSO-d_6): δ_C 34.8 ($C_6H_5CH_2S$), 52.2 (OCH_3), 126.5 (C2), 126.8 (C1), 127.4 (C4′), 128.5 (C2′ and C6′), 128.89–128.93 (C5, C6, and C3′ and C5′), 131.2 (C4), 135.8 (C1′), 143.5 (C3), 156.4 (NH=C(NH_2)$_2$), 165.3 (COOCH$_3$). MS (ES$^+$) m/z 316 ([M]$^+$, 100), (ES$^-$) m/z 350 ([M−H+Cl]$^-$, 100). Anal. Calcd for $C_{16}H_{18}N_3O_2SCl$: C, 54.6; H, 5.2; N, 11.9; S, 9.1; Cl, 10.1. Found: C, 54.7; H, 5.1; N, 12.0; S, 8.9; Cl, 10.4.

4.2.14. 4-Benzylmercapto-3-guanidino-benzoic acid (24). A solution of **23** (0.3 g, 0.85 mmol) in THF (1 mL) was added to 1 M NaOH (4 mL) and the mixture heated to 70 °C for 1 h. The solvent was evaporated, and the residue obtained re-dissolved in water (3 mL) and the pH adjusted to 6–7 with 1 M HCl. A solid slowly came out of solution, which was filtered and dried, yielding **24** as a white solid, (0.22 g, 87%): mp >260 °C (recryst from EtOH/water). ^{1}H NMR (DMSO-d_6): δ_H 4.23 (s, 2H, $C_6H_5CH_2S$), 7.21–7.41 (m, 6H, H5 and $C_6H_5CH_2S$), 7.62 (d, J = 1.5 Hz, 1H, H2), 7.76 (dd, J = 1.5 and 8.1 Hz, 1H, H6), 8.00* (br s, 4H, NH=C(NH_2)$_2$), 11.36* (br s, 1H, NH=C(NH_2)$_2$). ^{13}C NMR (DMSO-d_6): δ_C 35.6 ($C_6H_5CH_2S$), 126.9 (C2), 127.2 (C4′), 128.4 (C2′ and C6′), 128.7 (C5 and C6), 128.9 (C3′ and C5′), 131.7 (C1), 136.5, 137.2, 137.3 (C3, C4, C1′) 156.4 (NH=C(NH_2)$_2$), 169.5 (COOH). MS (ES$^+$) m/z 302 ([M+H]$^+$, 100), (ES$^-$) m/z 300 ([M−H]$^-$, 100). Anal. Calcd for $C_{15}H_{15}N_3O_2S{\cdot}H_2O$: C, 56.4; H, 5.4; N, 13.2; S, 10.0. Found: C, 56.3; H, 5.0; N, 13.2; S, 9.8.

4.2.15. Synthesis of 3-amino-4-benzylmercapto-benzoic acid (25). A mixture of **22** (0.42 g, 1.54 mmol), 1 M NaOH (3 mL) and MeOH (0.5 mL) was stirred at 40 °C for 8 h. The volume of the resulting solution was reduced to one third and the pH adjusted to 4 with 1 M HCl. The solution was extracted with EtOAc (30 mL) and the organic phase dried over anhydrous Na_2SO_4 and evaporated in vacuo, giving **25** as an off-white solid (0.35 g, 88%): mp 155–157 °C (recryst from MeOH). ^{1}H NMR ($CDCl_3$): δ_H 4.10 (s, 2H, SCH_2NC$_6$H$_5$), 5.45* (s, 2H, NH_2), 4.44 (2H, J = 5.6 Hz, $C_6H_5CH_2$NH), 7.03 (dd, J = 1.8 and 8.0 Hz, 1H, H6), 7.17–7.29 (m, 6H, $C_6H_5CH_2S$ and H5), 7.31 (d, J = 1.8 Hz, 1H, H2), 12.71* (br s, 1H, COOH). ^{13}C NMR (DMSO-d_6): δ_C 36.4 (SCH_2NC$_6$H$_5$) 114.6 and 116.9 (C1 and C6), 122.0 (C4), 126.9 (C4′), 128.2 (C2′ and C6′), 128.8 (C3′ and C5′), 130.1 (C1), 131.2 (C5), 137.4 (C1′), 147.7 (C3), 167.4 (COOH). MS (ES$^-$) m/z 258 ([M−H]$^-$, 100). Anal. Calcd for $C_{14}H_{13}NO_2S$: C, 64.8; H, 5.1; N, 5.4; S, 12.4. Found: C, 64.7; H, 5.0; N, 5.3; S, 12.2.

4.2.16. Methyl 4-benzylmercapto-3-[2-(9*H*-fluoren-9-ylmethoxycarbonylamino)-acetylamino] benzoate (26). To a solution of **22** (1 g, 3.7 mmol) in anhydrous DMF (5 mL) cooled in an ice bath were added Fmoc-Gly-OH (1.74 g, 5.9 mmol) and DCC (1.1 g, 5.5 mmol) and the mixture stirred for a few minutes on the ice bath and then at room temperature for 16 h. The suspended solid was removed by filtration and the filtrate evaporated in vacuo. The resulting residue was suspended in EtOAc (50 mL) and the insoluble material filtered out (solid A). The filtrate was chromatographed over a silica-gel column, starting with CH_2Cl_2 with an increasing gradient of CH_2Cl_2: EtOAc (up to 30% EtOAc). Fractions containing the product were combined with solid A and solvent removed in vacuo. Successive recrystallisations of the residue from EtOAc and EtOH yielded **26** as a white solid (0.65 g, 33%): mp 193–195 °C. ^{1}H NMR (DMSO-d_6): δ_H 3.83–3.88 (br s, 5H, OCH_3 and NHCOCH_2NHFmoc), 4.24–4.33 (m, 5H, $C_6H_5CH_2S$; CH and CH_2 Fmoc), 7.20–7.35 (m, 7H, $C_6H_5CH_2S$ and 2 C^{ar} H Fmoc), 7.42 (t, J = 7.3 Hz, 2H, 2 C^{ar} H Fmoc), 7.54 (d, J = 8.3 Hz, 1H, H5), 7.69–7.74 (m, 3H, H6 and 2 C^{ar} H Fmoc), 7.79* (app t, 1H, NHCOCH$_2$NHFmoc), 7.90 (d, J = 7.4 Hz, 2H, 2 C^{ar} H Fmoc), 8.11 (s, 1H, H2), 9.47* (s, 1H, NHCOCH$_2$NHFmoc). ^{13}C NMR (DMSO-d_6): δ_C 36.1 ($C_6H_5CH_2S$), 43.9 (NHCOCH$_2$NHFmoc), 46.5 (CH Fmoc), 52.0 (OCH_3), 65.8 (CH$_2$ Fmoc), 120.0 (CH Fmoc), 124.8 (C2), 125.1 (CH Fmoc), 125.9 (C6), 127.0 (CH Fmoc), 127.2 (C4′), 127.5 (CH Fmoc), 128.3 (C2′ and C5′), 128.6 (C5), 128.9 (C3′ and C5′), 135.22, 135.24, 136.2, 136.6 (C1, C3, C4 and C1′), 140.6 and 143.7 (2 × C^{quat} Fmoc), 156.5 (CO Fmoc), 165.6 (COOCH$_3$), 168.4 (NHCOCH$_2$NHFmoc). MS (ES$^+$) m/z 575 ([M+Na]$^+$, 100); (ES$^-$) m/z 551 ([M−H]$^-$, 100). HR-ES-MS (m/z) [M+Na]$^+$ calcd for $C_{32}H_{28}N_2O_5SNa$: 575.1611. Found: 575.1607.

4.2.17. 3-[(Aminoacetyl)amino]-4-benzylmercapto-benzoic acid (27). A solution of **26** (0.125 g, 0.23 mmol) in EtOAc (5 mL) and diethylamine (5 mL) was refluxed for 1 h and the resulting solution evaporated to dryness in vacuo. The resulting residue was suspended in MeOH (30 mL) and filtered. The filtrate was evaporated to dryness and the residue dissolved in THF (2 mL) and 1 M NaOH (4 mL), and refluxed for 1 h. The mixture was filtered and the pH adjusted to ~7 with 1 M HCl. The solid formed was collected by filtration and dried, giving **27** as a white solid (0.026 g, 36%): mp colour change to dark brown at 210 °C; melted at 240–241 °C. ^{1}H NMR (DMSO-d_6, TFA): δ_H 3.81–3.83 (br q, 2H, NHCOCH_2NH$_3^+$), 4.33 (s, 2H, $C_6H_5CH_2S$), 7.25–7.43 (m, 5H, $C_6H_5CH_2S$), 7.56 (d, J = 8.4 Hz, 1H, H5) 7.76 (dd, J = 1.7 and 8.4, 1H, H6), 7.94 (d, J = 1.6 Hz, 1H, H2), 8.17* (br s, 3H, NHCOCH$_2$NH_3^+), 10.07* (s, 1H, NHCOCH$_2$NH$_3^+$). ^{13}C NMR (DMSO-d_6): δ_C 35.9 ($C_6H_5CH_2S$), 40.9 (NHCOC H$_2$ NH$_3^+$), 126.9, 127.4 and 127.6 (C2, C5, C6, C4′), 128.2 (C2′ and C6′), 129.2 (C3′ and C5′), 134.0, 136.4 and 138.5 (C3, C4, C1′), 165.9 (NHCOCH$_2$NH$_3^+$), 166.8 (COOH). MS (ES$^-$) m/z 315 ([M−H]$^-$, 100). HR-ES-MS (m/z) [M−H]$^-$ calcd for $C_{16}H_{15}N_2O_3S$: 315.0802. Found: 315.0809.

4.3. Expression and purification of recombinant TcTS

The protocol for expression and purification of recombinant TcTS was adapted from Buschiazzo et al.[46]

Competent *E. coli* BL21(DE3)pLysS (Promega, Southampton, UK) cells were transformed with a plasmid containing the TcTS gene (pTrcTS611/2[47]) and grown overnight in LB broth containing 100 μg/mL ampicillin at 37 °C. The culture was diluted 1:50 with TB broth containing 100 μg/mL ampicillin and incubation continued under the same conditions to $A_{600} \sim 1.2$. The temperature was adjusted to 18 °C and bacteria induced to over-express recombinant TcTS by adding IPTG (1 mM). Induction was maintained for 14–16 h, after which cells were harvested and frozen. After one thaw/freeze cycle, lysis was achieved in the presence of 20 mM Tris–HCl, pH 8.5, 30 mM NaCl, 0.5% Triton X-100, 5 μg/mL DNAse I, protease inhibitor cocktail and lysozyme produced by the cells, followed by sonication (6×30 s pulses of ultrasound). The lysate was centrifuged at 16,000 rpm for 45 min at 4 °C and the supernatant subjected to iminodiacetic metal affinity chromatography (HisTrap FF 1 mL), on an AKTA-FPLC system (GE Healthcare, Little Chalfont, UK), after adjustment of the NaCl concentration to 0.5 M and pH to 8.5. After applying the lysate, the column was washed with buffer containing 20 mM Tris–HCl, pH 8.5, 0.5 M NaCl and 10 mM imidazole, and the protein eluted with a linear gradient of imidazole (10–500 mM) in the same buffer. Fractions containing the protein were desalted (HiPrep 26/10 desalting column) and further purification was achieved by FPLC anionic exchange (MonoQ 5/50 GL) applying a linear elution gradient of NaCl (0–0.5 M). Purified protein was quantified using the Bradford method, using BSA as a standard.[48]

4.4. Inhibition studies

Enzyme inhibition was assessed at I_{50} level using a continuous assay developed in our laboratory and described elsewhere.[11] The assay mixture, containing 20 mM Tris–HCl, pH 7.5, buffer, TcTS (10 μL of 0.33 mg/mL) and inhibitor solution (10 μL), was incubated for 10 min at 25 °C and reaction initiated by addition of MuNANA (10 μL of a 1 mM solution). The fluorescence of the released product (Mu) was monitored at 25 °C for 10 min, with excitation and emission wavelengths of 322 and 448 nm, respectively. Values of I_{50}, the concentration required to give 50% inhibition under the assay conditions described above, were determined by interpolation from a plot of assay velocity (in percentage of the activity in absence of inhibitors) versus inhibitor concentration, fitting to the IC_{50} 0–100 equation in Grafit[34] ($V = 100\%/\{1+([I]/I_{50})^s\}$), where s is a slope factor.

K_i determinations were performed using a discontinuous version of the assay. Briefly, the reaction mixture, containing 20 mM Tris–HCl, pH 7.5 (150 μL), enzyme solution (20 μL of 0.33 mg/mL) and, when studied, inhibitor solution (20 μL), was incubated for 10 min at 25 °C and reaction initiated by addition of MuNANA solution (10 μL of 2–20 mM MuNANA solution). After incubation (2, 3, 4 and 5 min), aliquots (40 μL) of the reaction mixture were taken and enzymatic reaction quenched by adding to 0.2 M Na_2CO_3 solution at pH 10 (100 μL) in a 96-well plate. The fluorescence of the released product (Mu) was measured at 25 °C with excitation and emission wavelengths of 365 and 442 nm, respectively. Inhibition type was assessed by analysing the patterns of three diagnostic classes of plot: $1/v_o$ versus $1/[S_o]$ for various [I]; $1/v_o$ versus [I] for various $[S_o]$; $[S_o]/v_o$ versus [I] at various $[S_o]$. Values of K_i and K_i' for mixed inhibition were determined by direct weighted ($1/v_o^2$ for weighting) least squares non-linear regression analysis of the raw data using the appropriate equation using the Grafit program,[34] viz., for mixed inhibition, $v = V_{max}[S_o]/([S_o](1 + [I]/K_i') + K_m(1 + [1]/K_i)$. Values of V_{max} and K_m were obtained by least squares non-linear regression analysis using Grafit.

Acknowledgments

We are grateful to Professor A. Carlos C. Frasch and Laura Ratier (Instituto de Investigaciones Biotecnológicas, Universidad Nacional de San Martín, Argentina) for general advice and to the Portuguese Foundation for Science and Technology (F.C.T.) for financial support.

References and notes

1. The World Health Report 2004: Changing history. 2004. Geneva, World Health Organization.
2. Cerecetto, H.; Gonzalez, M. *Curr. Top. Med. Chem.* **2002**, *2*, 1187–1213.
3. Vassena, C. V.; Picollo, M. I.; Zerba, E. N. *Med. Vet. Entomol.* **2000**, *14*, 51–55.
4. Schenkman, S.; Jiang, M. S.; Hart, G. W.; Nussenzweig, V. *Cell* **1991**, *65*, 1117–1125.
5. Schenkman, S.; Eichinger, D.; Pereira, M. E. A.; Nussenzweig, V. *Annu. Rev. Microbiol.* **1994**, *48*, 499–523.
6. Ming, M.; Chuenkova, M.; Ortegabarria, E.; Pereira, M. E. A. *Mol. Biochem. Parasitol.* **1993**, *59*, 243–252.
7. Buschiazzo, A.; Tavares, G. A.; Campetella, O.; Spinelli, S.; Cremona, M. L.; Paris, G.; Amaya, M. F.; Frasch, A. C. C.; Alzari, P. M. *EMBO J.* **2000**, *19*, 16–24.
8. Cross, G. A. M.; Takle, G. B. *Annu. Rev. Microbiol.* **1993**, *47*, 385–411.
9. Cremona, M. L.; Campetella, O.; Sanchez, D. O.; Frasch, A. C. C. *Glycobiology* **1999**, *9*, 581–587.
10. Buschiazzo, A.; Amaya, M. F.; Cremona, M. L.; Frasch, A. C.; Alzari, P. M. *Mol. Cell* **2002**, *10*, 757–768.
11. Neres, J.; Buschiazzo, A.; Alzari, P. M.; Walsh, L.; Douglas, K. T. *Anal. Biochem.* **2006**, *357*, 302–304.
12. Schenkman, S.; de Carvalho, L. P.; Nussenzweig, V. *J. Exp. Med.* **1992**, *175*, 567–575.
13. Vandekerckhove, F.; Schenkman, S.; de Carvalho, L. P.; Tomlinson, S.; Kiso, M.; Yoshida, M.; Hasegawa, A.; Nussenzweig, V. *Glycobiology* **1992**, *2*, 541–548.
14. Paris, G.; Ratier, L.; Amaya, M. F.; Nguyen, T.; Alzari, P. M.; Frasch, A. C. C. *J. Mol. Biol.* **2005**, *345*, 923–934.
15. Watts, A. G.; Damager, I.; Amaya, M. L.; Buschiazzo, A.; Alzari, P.; Frasch, A. C.; Withers, S. G. *J. Am. Chem. Soc.* **2003**, *125*, 7532–7533.
16. Watts, A. G.; Oppezzo, P.; Withers, S. G.; Alzari, P. M.; Buschiazzo, A. *J. Biol. Chem.* **2006**, *281*, 4149–4155.
17. Amaya, M. F.; Buschiazzo, A.; Nguyen, T.; Alzari, P. M. *J. Mol. Biol.* **2003**, *325*, 773–784.
18. Agusti, R.; Paris, G.; Ratier, L.; Frasch, A. C. C.; de Lederkremer, R. M. *Glycobiology* **2004**, *14*, 659–670.
19. Previato, J. O. *Glycobiology* **2004**, *14*, 25G.

20. Streicher, H.; Busse, H. *Bioorg. Med. Chem.* **2006**, *14*, 1047–1057.
21. Ferrero-Garcia, M. A.; Sanchez, D. O.; Frasch, A. C. C.; Parodi, A. J. *An. Asoc. Quim. Argent* **1993**, *81*, 127–132.
22. Streicher, H. *Curr. Med. Chem.: Anti-infective Ag* **2004**, *3*, 149–161.
23. Chand, P.; Babu, Y. S.; Bantia, S.; Chu, N. M.; Cole, L. B.; Kotian, P. L.; Laver, W. G.; Montgomery, J. A.; Pathak, V. P.; Petty, S. L.; Shrout, D. P.; Walsh, D. A.; Walsh, G. W. *J. Med. Chem.* **1997**, *40*, 4030–4052.
24. Chand, P.; Kotian, P. L.; Morris, P. E.; Bantia, S.; Walsh, D. A.; Babu, Y. S. *Bioorg. Med. Chem.* **2005**, *13*, 2665–2678.
25. Howes, P. D.; Cleasby, A.; Evans, D. N.; Feilden, H.; Smith, P. W.; Sollis, S. L.; Taylor, N.; Wonacott, A. J. *Eur. J. Med. Chem.* **1999**, *34*, 225–234.
26. Jedrzejas, M. J.; Singh, S.; Brouillette, W. J.; Laver, W. G.; Air, G. M.; Luo, M. *Biochemistry* **1995**, *34*, 3144–3151.
27. Williams, M.; Bischofberger, N.; Swaminathan, S.; Kim, C. U. *Bioorg. Med. Chem. Lett.* **1995**, *5*, 2251–2254.
28. Goodford, P. J. *J. Med. Chem.* **1985**, *28*, 849–857.
29. Atigadda, V. R.; Brouillette, W. J.; Duarte, F.; Ali, S. M.; Babu, Y. S.; Bantia, S.; Chand, P.; Chu, N.; Montgomery, J. A.; Walsh, D. A.; Sudbeck, E. A.; Finley, J.; Luo, M.; Air, G. M.; Laver, G. W. *J. Med. Chem.* **1999**, *42*, 2332–2343.
30. Brouillette, W. J.; Atigadda, V. R.; Luo, M.; Air, G. M.; Babu, Y. S.; Bantia, S. *Bioorg. Med. Chem. Lett.* **1999**, *9*, 1901–1906.
31. Ewing, T. J. A.; Makino, S.; Skillman, A. G.; Kuntz, I. D. *J. Comput. Aided Mol. Des.* **2001**, *15*, 411–428.
32. Singh, S.; Jedrzejas, M. J.; Air, G. M.; Luo, M.; Laver, W. G.; Brouillette, W. J. *J. Med. Chem.* **1995**, *38*, 3217–3225.
33. Mehta, A.; Jaouhari, R.; Benson, T. J.; Douglas, K. T. *Tetrahedron Lett.* **1992**, *33*, 5441–5444.
34. Grafit 5.0. Erithacus Software Limited. Horley, Surrey, UK, 2005.
35. Kim, C. U.; Lew, W.; Williams, M. A.; Liu, H. T.; Zhang, L. J.; Swaminathan, S.; Bischofberger, N.; Chen, M. S.; Mendel, D. B.; Tai, C. Y.; Laver, W. G.; Stevens, R. C. *J. Am. Chem. Soc.* **1997**, *119*, 681–690.
36. von Itzstein, M.; Wu, W. Y.; Kok, G. B.; Pegg, M. S.; Dyason, J. C.; Jin, B.; Phan, T. V.; Smythe, M. L.; White, H. F.; Oliver, S. W.; Colman, P. M.; Varghese, J. N.; Ryan, D. M.; Woods, J. M.; Bethell, R. C.; Hotham, V. J.; Cameron, J. M.; Penn, C. R. *Nature* **1993**, *363*, 418–423.
37. Sudbeck, E. A.; Jedrzejas, M. J.; Singh, S.; Brouillette, W. J.; Air, G. M.; Laver, W. G.; Babu, Y. S.; Bantia, S.; Chand, P.; Chu, N.; Montgomery, J. A.; Walsh, D. A.; Luo, M. *J. Mol. Biol.* **1997**, *267*, 584–594.
38. Babu, Y. S.; Chand, P.; Bantia, S.; Kotian, P.; Dehghani, A.; El Kattan, Y.; Lin, T. H.; Hutchison, T. L.; Elliott, A. J.; Parker, C. D.; Ananth, S. L.; Horn, L. L.; Laver, G. W.; Montgomery, J. A. *J. Med. Chem.* **2000**, *43*, 3482–3486.
39. Amaya, M. F.; Watts, A. G.; Damager, T.; Wehenkel, A.; Nguyen, T.; Buschiazzo, A.; Paris, G.; Frasch, A. C.; Withers, S. G.; Alzari, P. M. *Structure* **2004**, *12*, 775–784.
40. RCSB Protein Data Bank, http://www.rcsb.org/.
41. Vriend, G. *J. Mol. Graph.* **1990**, *8*, 52–56.
42. Sybyl 6.8. Tripos Inc., 2002.
43. Naim, S. S.; Singh, S. K.; Sharma, S.; Gupta, S.; Fatma, N.; Chatterjee, R. K.; Katiyar, J. C. *Indian J. Chem. B* **1988**, *27*, 1106–1109.
44. Göker, H.; Tebrizli, E.; Abbasoglu, U. *Il Farmaco* **1996**, *51*, 53–58.
45. Donleavy, J. J.; Condit, P. C. *J. Am. Chem. Soc.* **1947**, *69*, 1781–1784.
46. Buschiazzo, A.; Frasch, A. C. C.; Campetella, O. *Cell. Mol. Biol.* **1996**, *42*, 703–710.
47. Buschiazzo, A.; Campetella, O.; Frasch, A. C. C. *Glycobiology* **1997**, *7*, 1167–1173.
48. Bradford, M. M. *Anal. Biochem.* **1976**, *72*, 248–254.